CFD-DEM BASED DESIGN OF ELBOW LIFTING PIPE CONVEYANCE UNDER NEGATIVE PRESSURE AIRFLOW
/
基于 CFD-DEM 的负压气流下弯头提升管道输送设计

Lianglong ZHANG[1)], Yue SUN[1)], Fan Yang[1)], Yalin Sun[1)], Fangyan Wang [1,3*)]; Xin Wang[2*)]

[1)] College of Mechanical and Electrical Engineering, Qingdao Agricultural University, Qingdao 266109, China.

[2)] College of Civil Engineering and Architecture, Qingdao Agricultural University, Qingdao 266109, China.

[3)] Collaborative Innovation Center for Shandong s Main Crop Production Equipment and Mechanization, Qingdao 266109, China.

[*] *Corresponding authors, Email: wfy 66@163.com*

DOI: https://doi.org/10.35633/inmateh-75-46

Keywords: *chili cleaning, bend lift conveyor, conveying efficiency, CFD-DEM*

ABSTRACT

To improve the material conveying efficiency in the elbow lifting transportation process under negative pressure airflow and to solve pipeline material blockage issues, a chili cleaning device was used as the core model. CFD-DEM coupled simulation was employed to analyze the lifting process of non-spherical chili materials in the elbow pipe. Key parameter optimization was carried out through experimental design, determining the optimal parameter combination as a pipeline curvature of 2.03 and an air-to-feed ratio of 4.571. This combination achieved a conveying efficiency 4.406 times higher than the lowest efficiency case, and the uniformity of material transport under optimal parameters was verified through simulation. This study lays a solid foundation for the design of pipeline bends and the optimization of material conveying analysis.

摘要

为提高负压气流下弯管抬升输送过程物料输送效率，解决管道物料堵塞。以辣椒清选装置为核心模型，采用 CFD-DEM 耦合模拟，分析非球形辣椒物料弯管的提升过程。通过试验设计进行关键参数优化，确定最佳参数组合为管道曲率 2.03 和气送比 4.571。该组合的输送效率是最低效率情况下的 4.406 倍，并通过仿真验证了最佳参数组合下物料输送的均匀性。这为设备弯管的设计和物料输送分析的优化奠定了坚实的基础。

INTRODUCTION

Pneumatic conveying originated in Britain in the late 19th century. Since then, it has been extensively applied in diverse industries. Pneumatic conveying systems enjoyed a global market of nearly 30 billion U.S. dollars in 2021 *(Hentschel, 2011; Hilgraf, 2023).* Compared to traditional conveying methods, pneumatic conveying is characterized by high efficiency and low cost. With the continuous advancement of the industry, the demands for its conveying efficiency and performance are constantly escalating. However, pipeline conveying is merely a simple component of the device, which, therefore, lacks sufficient attention. This oversight seriously impacts the overall efficiency and operational effectiveness *(Afkhami et al., 2015; Cong et al., 2018; Ma & Zhao, 2018).*

Pneumatic conveying technology did not attract scholars' attention until the 1950s, although it was developed earlier in overseas countries. During the continuous development of pneumatic conveying technology industry, pneumatic conveying can be mainly categorized into dilute-phase pneumatic conveying, dense-phase dynamic pressure pneumatic conveying, dense-phase hydrostatic pneumatic conveying, and cylinder pneumatic conveying, among which dilute-phase pneumatic conveying methods are currently the most widely adopted. The existing analysis is primarily focused on spherical particles, simply constrained to the theoretical analysis of horizontal conveying or lifting conveying. With the gradual development of equipment in the multi-level direction, pneumatic pipeline is no longer limited to horizontal conveying, so there is an urgent need to provide theoretical support for the design of vertical-horizontal lifting.

Lianglong Zhang, postgraduates; Yue Sun, postgraduates; Fan Yang, Lecturer, Ph.D.; Yalin Sun, postgraduates; Fangyan Wang, professor, Ph.D.; Xin Wang, Lecturer, Ph.D.

Traditionally, design mode requires a lot of human and material resources. The coupled fluid mechanics and discrete element simulation technique, on the other hand, help to reduce the consumption of resources and is able to track and analyze the motion state of materials under the action of fluid from a microscopic perspective, which, hence, has been widely used in various types of pneumatic research. For example, Li Zhengquan and Chen Huimin analyzed the force between particles and pipe wall and the scouring effect on the pipe wall in pipelines using fluid mechanics and discrete element method *(Li et al., 2024)*. Gu Fengwei and Zhao Youqun analyzed the conveying device of straw no-tillage planter with the help of CFD-DEM coupled simulation and improved the homogeneity of straw casting and crushing *(Gu et al., 2022).* Combining computational fluid dynamics and discrete element method, Hemin Zhao and Yongzhi Zhao effectively simulated the motion state of particles in horizontal channel pneumatic conveying *(Zhao & Zhao, 2020).* In summary, the reliability and applicability of the coupled CFD-DEM simulation technique have been fully verified. However, vertical-horizontal lifting process is rarely explored, and most of the existing research focuses on regular particles and lacks actual data to provide a basis for pipeline design.

By constructing a CFD-DEM coupled simulation model using chili peppers and chili pepper stalks as particle models, this paper investigates the conveying process of vertical-horizontal lifting in depth from the laws of air flow field and the motion state of particles and studies the conveying effect of materials under different structures *(Chen et al., 2020; Uzi & Levy, 2018).* Combined with the experimental design, the optimal structure parameters are identified through experiments and simulation verification *(Drescher et al., 2025).* The research results of this paper will provide valuable reference for the subsequent material lifting and conveying system and its structural design.

MATERIALS AND METHODS

Installations and Critical Areas

On the basis of previous research on chili cleaning device, this paper analyzed bending and lifting pipe of the chili mixture. The device consisted of conveyor belt, rotary feeder, conveyor pipe, rotary unloader, settling pipe and other components, as detailed in Fig. 1. Among them, the specific gravity sorting area (Fig. 1 (a)) and the inertia sorting area (Fig. 1 (b)) played the most critical role in operation. The chili was transported through the vertical-horizontal lifting pipe and then mixed. The detailed analysis will be performed in this paper to maximize the conveying efficiency and ensure the uniformity of conveying.

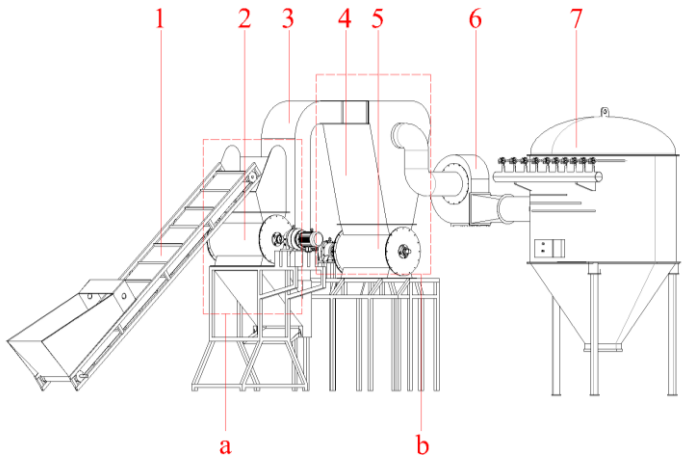

Fig. 1 - Chilli separator

1. conveyor belt; 2. rotary feeder; 3. lifting air duct; 4. sorting device; 5. rotary unloader; 6. centrifugal fan; 7. settling box
a. Specific gravity sorting area; b. Inertia sorting area

Theoretical analysis

The conveying pipeline needed to be rationally arranged, whose conveying efficiency would otherwise be affected, thereby potentially resulting in blockages, etc. Vertical - horizontal lifting pipelines are mainly divided into six types, as shown in Fig. 2 (a), where Pipeline *4* is the theoretically optimal route, which, however, is difficult to achieve in practice. Pipeline *2* is currently the most commonly used as it can be installed in a more standardized layout. Pipeline *2* has some single rounded corners designed into two rounded corners, which results in increased dissipation. Therefore, this paper presents an in-depth analysis and design of Pipeline *2*.

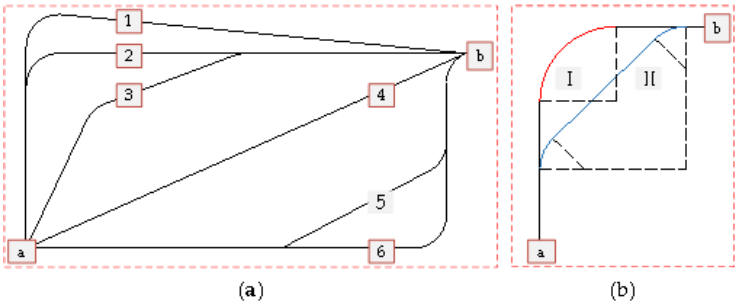

Fig. 2 - Pneumatic lifting conveying lines

a. Pneumatic lifting of the conveying pipeline arrangement; b. Schematic diagram of multiple corners of the pipeline

Conveying air velocity

Air velocity is one of the key parameters of chili cleaning device. According to the relevant provisions of the pipeline layout of the design institute, in the case of vertical or inclined pipe with elbows, the conveying air velocity should be 2.4 to 4.0 times the suspension velocity of the material. The floating speed of the material, V_P, was measured using suspension test bench provided by Qingdao Agricultural University *(Gao et al., 2012; Ma Z. et al., 2011)*, as listed in Table 1.

Table 1

Mixture material conveying speed

	Overall dimensions [mm]	Suspension speed [m·s^{-1}]	Conveying air velocity [m·s^{-1}]
Chili	52.4~98.2	12.2-14.4	29.28~57.6
Chili stalks	21.5~43.1	9.1-10.5	21.84~42
Fractured stone	8~13	14.8~17.9	35.52~71.6

As the specific gravity sorting area is responsible for sorting out heavier impurities such as stones from the chili mixture, the conveying air velocity needs to be less than the minimum counterpart of stones and to meet the requirements in the conveying speed of chili peppers, stalk and other materials. Therefore, the optimal conveying air velocity of negative pressure at the inlet is 29.28~35.52 m·s^{-1}.

Curvature of bent pipe

The influence of the curvature generated in the material conveying process on the trajectory of the material was discussed.

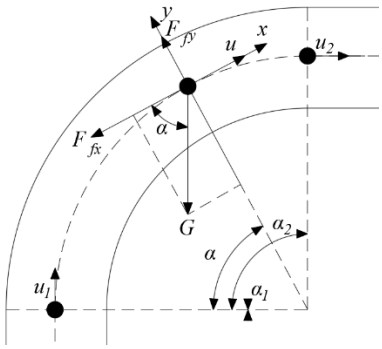

Fig. 3 - Material Bend Motion Analysis

The equations of motion are:

$$\begin{cases} -F_{\text{fx}} - G\cos\alpha = ma_x \\ F_{\text{fy}} - G\sin\alpha = ma_y \end{cases} \quad (1)$$

where F_{fx}, F_{fy} - airflow resistance components, (N); G - gravity, (N).

According to the boundary conditions, when particles were at Position 1, the angle of motion between the particles and the elbow was α_1=0°, and the velocity of the particles entering the bending phase was assumed to be $u=u_1$; when particles were at Position 2, the angle of motion between the particles and the elbow was α_2=90°, and the velocity of the particles entering the bending phase was assumed to be $u=u_2$.

The relationship between u_2 and α can be described as:

$$u_2^2 - e^{-f_w\alpha}u_1^2 = e^{-\mathrm{fw}\alpha}\frac{2\mathrm{gR}}{4f_w^2+1}\{3f_w + e^{2f_w\alpha}[2(f_w^2-1)\sin\alpha - 3f_w\cos\alpha]\} \quad (2)$$

The final simplification of the above equation is obtained by combining the particles as they move from position 1 to position 2:

$$u_2 = e^{-\frac{\pi}{2}\mathrm{fw}}\sqrt{u_1^2 + \frac{2\mathrm{gR}}{4f_w^2+1}[3f_w + e^{\pi f_w}(2f_w^2-1)]} \quad (3)$$

From eq. 3, it can be seen that the velocity of material movement is affected by the bending radius of the pipe.

Shape of Pipe

Pipes are commonly rectangular, circular and oval. Among them, circular pipes are more widely used for horizontal conveying. However, since the vertical-horizontal lifting process is very complex, this paper will examine and compare these three types of pipes in depth.

Gas-to-feed ratio

In the material conveying process, the material is vertically lifted and then horizontally conveyed through bending pipes. According to the relevant provisions about pipeline arrangement offered by the design institute, the air velocity of the material conveyed is mostly in the range of 12 m/s to 40 m/s, which is in line with the dilute phase pneumatic conveying speed conditions *(Du et al., 2014; Huo et al., 2013).* Under the condition of dilute-phase pneumatic conveying, gas-to-feed ratio is required to be between 1 and 5 *(Hongxun, 1993),* so as to meet the process requirements and performance indexes of the whole conveying system.

Experimental factors

Based on the above comprehensive analysis, the main factors affecting the material in the state of vertical-bend-horizontal conveying included pipe type, bend radius R, gas-to-feed ratio C. Curvature R/D was associated with elbow size, but was represented by radius R instead as the negative pressure of the pipe was constant and the cross-section size of the pipe had been determined. It will be further analyzed as a key influencing factor.

Simulation Settings

The simulation was coupled with ANSYS 2021r1 and EDEM 2020 software. The 'Mesh' module in ANSYS 2021r1 was used to delineate the mesh, and the Fluent module to analyze the flow field. In the Fluent module, the fluid medium was set to be air, and the k-ε model was employed to calculate the transient simulation method. The SIMPLE algorithm was used for computation. The material particles were generated and the mechanism was modelled using EDEM software. Data exchange between the two software packages was facilitated through a coupling plug-in, ensuring the accuracy and efficiency of the entire simulation *(Alihosseini, Saegrov, & Thamsen, 2019; Zhao L. et al., 2016).*

Simulation of particles and geometrical models

1) Particle physical parameters and contact parameters;

The physical properties of the chili mixture were measured based on the statistical principles of the physical parameters of the harvested chili mixtures. The characteristic properties of the material that could not be measured directly were obtained by EDEM calibration *(Zhang et al., 2023).* The parameters and contact coefficient of the material are listed in Table 2.

Table 2

Physical parameters of the material

	Poisson's ratio	Shear modulus [MPa]	Density [kg·m^{-3}]
Chili	0.31	3.12	817.13
Chili handle	0.43	1.35	1024.45
Steel	0.29	79920	7860
	Coefficient of recovery	Coefficient of static friction	Coefficient of kinetic friction
Chili peppers-chili peppers	0.372	0.364	0.272
Chili peppers-chili stalks	0.277	0.452	0.341
Chili - steel	0.413	0.491	0.233
Chili stalk - chili stalk	0.362	0.682	0.578
Chili - steel	0.335	0.538	0.452

2) Particle modeling

In order to accurately simulate the actual working effect of the pipeline, particle modeling was conducted at a ratio of 1:1 between chili and chili stalk. By employing the SolidWorks finite element mesh module, the model was divided to generate node coordinates, and then the data was imported into EDEM software to construct the model for the particles of chili and chili stalk, as shown in Fig. 4.

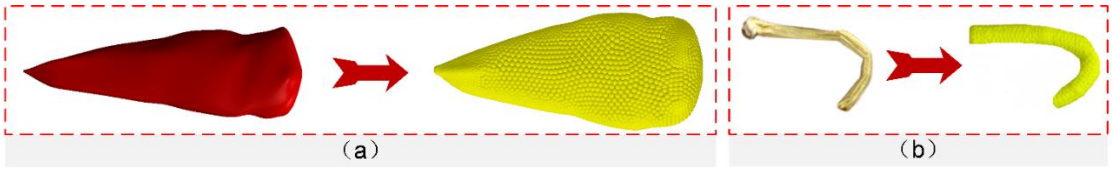

Fig. 4 - Particle-filled models

a. Chili filler model; b. Chili stem filler model

3) Geometric modeling

A geometric model was established by SolidWorks software, and the mesh was delineated by the 'Mesh' module in Workbench, as shown in Fig. 5.

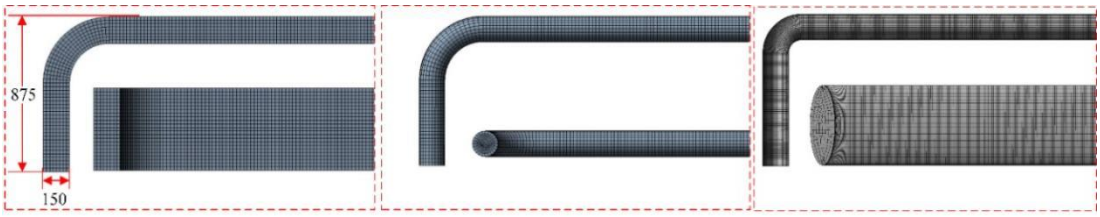

Fig. 5 - Geometric Modeling Mesh

Experimental

1) One-way test;

Using CFD-DEM coupled simulation technology and taking the uniformity of the airflow field, the stability of material conveying and the conveying efficiency as the evaluation indexes, this paper conducted the single-factor simulation analysis for the three key parameters, namely pipe type, curvature of elbow pipe *R/D* and air-to-feed ratio *C*. Among them, the pipe type included round, rectangular and oval; the curvature of elbow pipe *R/D* was set to be (1 ~ 5) because of common small curvature *R/D* = 2 and large curvature *R/D* = 5, and air-to-feed ratio *C* to be (1 ~ 5) according to the conditions of the rarefied-phase pneumatic conveying.

2) Orthogonal test;

According to the one-factor simulation results and agronomic requirements, curvature X_1 and air-to-feed ratio X_2 were taken as test factors, and material conveying efficiency *Y* as the evaluation standard (set 1s conveying 100 chilies as the unit efficiency). With the help of Design-Expert, two-factor three-level orthogonal test was performed *(Cong et al., 2018).*

The test factors are detailed in Table 3.

Table 3

Factor level coding table for chili pepper scavenging device test

Encodings	Experimental factors	
	Curvature X_2	Gas to material ratio X_3
-1	1	1
0	2	3
1	3	5

In order to ensure the reliability of the CFD-DEM simulation, the optimal structural parameters were firstly obtained by simulation and experimental design analysis, and the pipe was processed according to the optimal combination of parameters to carry out the bending and lifting test on chili and chili stalk. During the test, the velocity at the key entrance and exit nodes was measured by a pipeline airflow speed transmitter, and compared with the velocity at the same locations obtained during the simulation to assess the reliability of the simulation results.

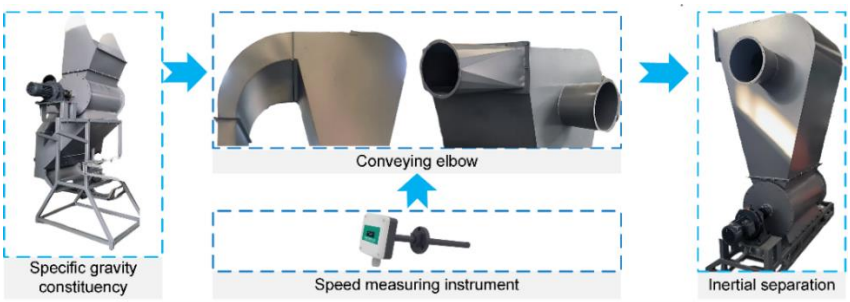

Fig. 6 - Of actual test setup

RESULTS

Analysis of the results of the one-way test

Analysis of pipe type simulation results

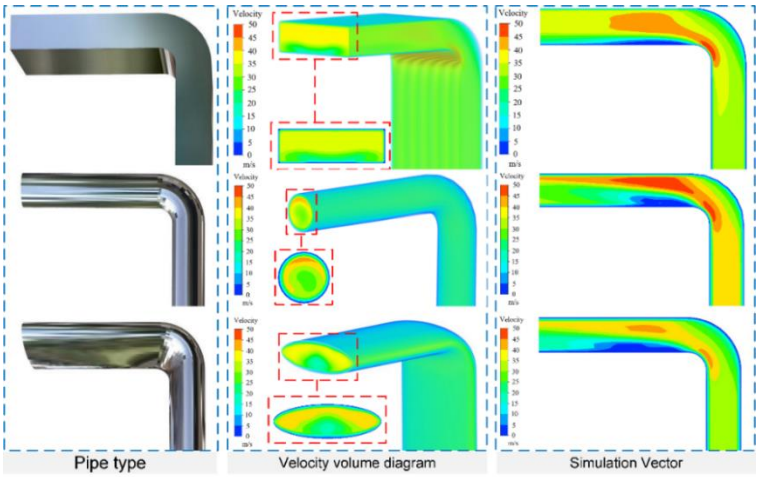

Fig. 7 - Pipeline fluid simulation volume diagram

As can be seen from the analysis of the cloud images for three types of elbow shown in Figure 7, airflow moved from the vertical area to the turning area in circular and elliptical elbows, mainly concentrating at the bottom and converging upward, which resulted in the turbulence in the horizontal area and therefore made it difficult to *ensure the uniformity of material transportation (Liu et al., 2024; Wang et al., 2024; Zhang & Newell, 2024)*. In contrast, airflow movement in most areas remained unaffected when the airflow passed through the turning area in rectangular elbow due to the limitation of its own structure, so that airflow remained relatively stable in the material transportation process in the rectangular elbow, providing favorable conditions for the uniform and orderly transportation of the material.

Therefore, in terms of the airflow in the vertical and horizontal conveying processes, rectangular pipe was superior to oval and round ones. In the turning area, turbulence would not be produced in the rectangular pipe, which effectively ensured uniform airflow in the material conveying process and more stable airflow within the rectangular pipe from vertical to horizontal conveying.

Analysis of curvature simulation

The rectangular pipe was simulated, with air-to-feed set to be 2 and curvature *R/D* to be 1, 2, 3 and 4, respectively *(Zhou et al., 2016).*The simulation results are illustrated in Fig. 8.

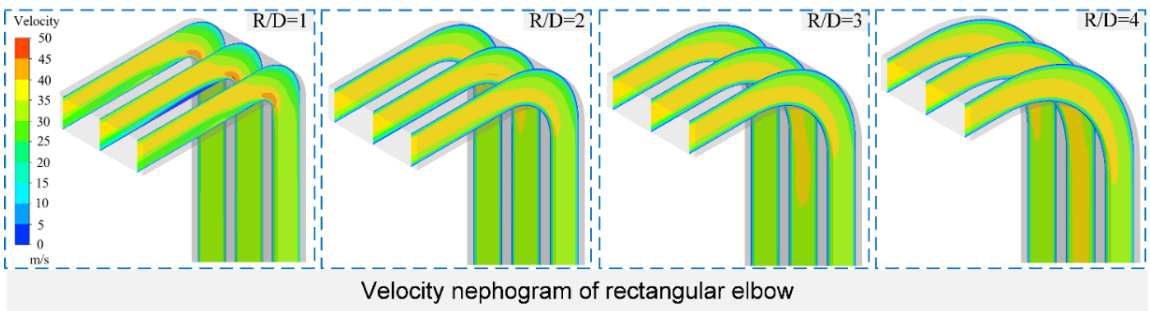

Fig. 8 - Curvature fluid simulation vector diagram

a. Velocity nephogram of rectangular elbow; b. Velocity nephogram of circular bend

As can be seen from Fig. 8, with the increase of the curvature *R/D*, the horizontal area of rectangular and round pipes did not change significantly, while the vertical area of high-velocity airflow area continued to expand towards the inlet.

As in the presence of negative pressure, when the airflow passes through the turning area, it would be attached to the lower wall of the turning area under the action of the Coanda Effect, thus generating adhesive flow. With the gradual increase of the curvature *R/D*, the turning trend of the airflow became more gentle and the adhesive flow of the steering process was cushioned. As a result, the high-velocity flow area was extended. Therefore, the larger the curvature *R/D*, the smoother the flow in the turning region.

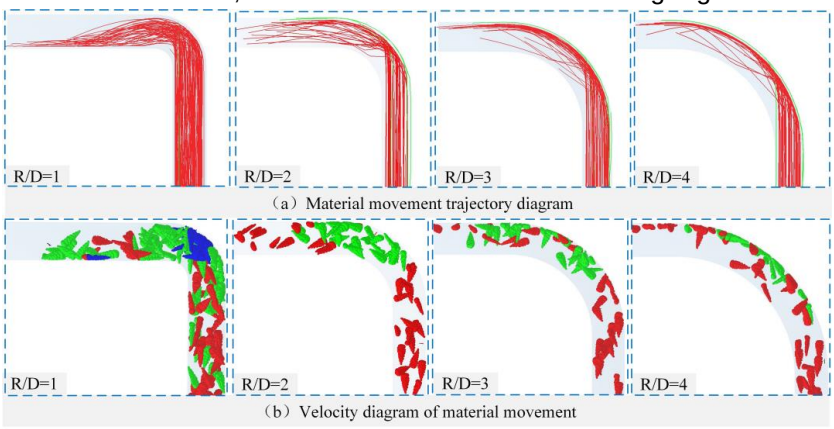

Fig. 9 - Particle coupling effect

a. Material movement trajectory diagram; b. Velocity diagram of material movement

As can be seen from Fig. 9, the larger the curvature *R/D*, the trajectory of the material was gradually concentrated at the top upon the completion of vertical and horizontal conveying. If a large number of materials were concentrated at the top of the pipe, then they would be unevenly distributed within the pipe, thus lowering the material conveying efficiency.

With the gradual increase of the curvature *R/D*, the number of collisions of material trajectory in the turning area obviously increased. The material would collide with the upper wall of the elbow under the action of the upward movement inertia when moving from the vertical area to the turning area. In addition, the turning area was enlarged, so that the materials would continue to collide repeatedly with the turning area following their initial collision, making the pipe very likely to be blocked.

For the sake of a comprehensive comparison, among the four common curvatures of rectangular pipes, the curvature *R/D* = 2 helped to ensure the uniform distribution of the materials in the pipe after they passed through the turning area and to effectively reduce the number of collisions between the materials as well as between the materials and the pipe wall, thus reducing the degree of damage to the materials.

Influence of air/feed ratio on conveying performance

A rectangular bend was simulated, with the curvature R/D being set to 2 and air-to-feed ratio to 1, 2, 3, 4 and 5, respectively (*Ebrahimi & Crapper, 2017*). The corresponding simulation results are shown in Fig. 10.

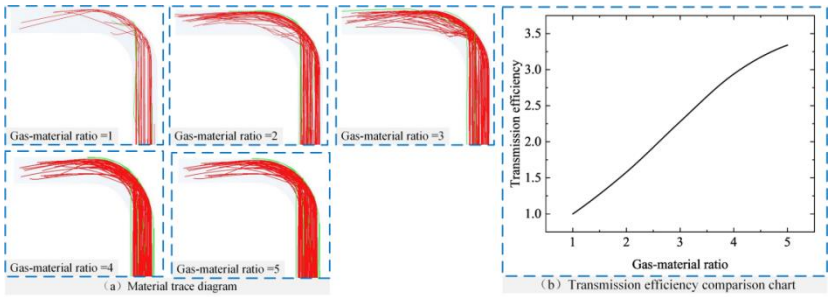

Fig. 10 - Particle coupling trace diagram

a. Material trace diagram; b. Transmission efficiency comparison chart

As seen in Fig. 10(a), increasing the air-to-feed ratio improved the uniformity of material conveying. With a higher air-to-feed ratio, the materials initially accumulated in the turning area, causing a reduction in speed. However, as the materials moved into the horizontal conveying section, they formed a more stable mass, leading to a more uniform trajectory.

As seen in Fig. 10(b), at a low air-to-feed ratio, the materials were not conveyed rapidly due to the occurrence of a winding phenomenon. As the air-to-feed ratio gradually increased, the cross-sectional area of the material exposed to the airflow became larger, enhancing the pulling force of the air on the material surface. This resulted in accelerated movement of the materials, thereby improving the efficiency of material conveying.

Analysis of orthogonal test

Experimental design and analysis were conducted using Design-Expert 13 software, with transportation efficiency as the evaluation indicator. The transportation efficiency of the least efficient combination was set as the baseline unit, represented as Y_1=1. The efficiency of the remaining combinations was then expressed as a multiple of the baseline according to the simulation results, i.e., $Y_1=n\times1(n\geq1)$. The experimental results and ANOVA analysis are presented in Tables 4 and 5, respectively.

Table 4

Relationship between conveyor airflow speed and suspension velocity

Serial number	Factors		Performance indicators
	Curvature X_1	Gas-to-feed ratio X_2	Gas to material ratio Y_1
1	2	1	3.2
2	1	3	1.53
3	1	5	2.21
4	2	3	3.41
5	2	3	3.67
6	3	1	1.21
7	2	3	3.98
8	2	5	4.12
9	3	5	3.96
10	1	1	1
11	2	3	3.87
12	3	3	2.27

Table 5

ANOVA table for conveying efficiency

Source of variance	Square sum	Degrees of freedom	Mean square	*F*	*P*	Significance
Modelling	15.13	5	3.03	32.25	0.0001	Significant
X_1	1.21	1	1.21	12.95	0.0088	Significant
X_2	3.97	1	3.97	42.29	0.0003	Significant
X_1X_2	0.5929	1	0.5929	6.32	0.0402	Significant
X_2^1	8.15	1	8.15	86.82	< 0.0001	extremely significant
X_2^2	0.005	1	0.005	0.0529	0.8246	Insignificant
Residual	0.657	7	0.0939			
Lost proposal	0.4538	3	0.1513	2.98	0.1597	Insignificant
Inaccuracies	0.2032	4	0.0508			
Aggregate	15.79	12				

As shown in Table 6, the fit of the conveyor efficiency model was significant (p<0.1), while the out-of-fit term was insignificant (p = 0.1597, p>0.05). The terms X_1, X_2, and X_1X_2 had a significant effect on the chili clearing rate, with X_2^1 being extremely significant. After excluding the insignificant regression terms, the regression equation for conveying efficiency can be expressed as:

$$Y = 3.72 - 0.45X_1 - 0.8133X_2 - 0.3850X_1X_2 - 1.72{X_1}^2 \quad (4)$$

Air-to-feed ratio had a greater impact on material conveying efficiency than curvature. The interaction between air-to-feed ratio and curvature had a significant effect on conveying efficiency.

To determine the optimal levels of test factors, the optimization module of Design-Expert 13 software was used to establish a parameter optimization mathematical model. The model aimed to maximize conveying efficiency while considering the boundary conditions of each factor's test values. The objective function and constraints are as follows:

$$\begin{cases} \max Y(X1,\ X2) \\ \text{s.t} \begin{cases} 1 \le X1 \le 3 \\ 1 \le X2 \le 5 \end{cases} \end{cases} \tag{5}$$

According to the analysis, the optimal parameter combination was a curvature of 2.03 and an air-to-feed ratio of 4.571, resulting in a unit material conveying efficiency of up to 4.406.

Optimal combination of experimental and simulation results and comparison

Optimal simulation results

The simulation analysis results are shown in Fig. 11. As the materials were lifted from the vertical area to the turning area and then into the horizontal area, they were transported along the upper wall of the horizontal section due to changes in air resistance and gravity acting in the downward movement direction. Eventually, if the materials did not fall to the lower wall of the horizontal section, a uniform motion flow was formed, enabling stable horizontal conveying of the materials.

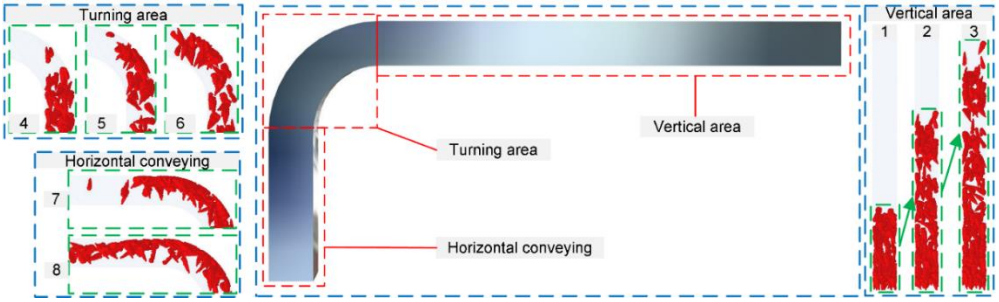

Fig. 11 - Schematic diagram of the motion state of the coupled simulated particles

Actual test results and simulation verification

The actual test was carried out in Jiaozhou, Qingdao, with a rectangular pipe shape, small curvature *R/D* = 2.03, and an air-to-feed ratio of 4.571. The materials used were chili peppers and chili stalks in the ratio of 10:1. The components of the test setup included an inertial sorting device, a centrifugal fan, and a curved conveying pipe.

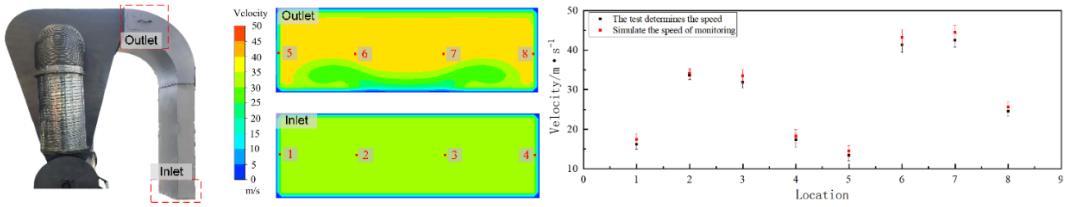

Fig. 12 - Comparison of actual test and simulation key position speed intention

As shown in Fig. 12, by comparing the simulation results of the velocity at the same positions at the inlet and outlet with the actual measurement results, it was found that the actual velocity was slightly lower than the simulated one. This deviation remained within a reasonable range due to the increasing energy consumption of airflow and material flow under the influence of external environmental factors in practical applications. Since the simulated speed closely matched the actual speed in both trend and magnitude, the simulation test results were proven to be highly accurate and reliable.

CONCLUSIONS

In this paper, the CFD-DEM coupled simulation technique was employed to simulate the material lifting and conveying state in a vertical-bend-horizontal pipeline. To achieve optimal material lifting and conveying efficiency, simulation analyses were conducted on pipe type, curvature, and air-to-feed ratio. Combined with

experimental design, the optimal pipe structure was determined to maximize material conveying efficiency. The following conclusions can be drawn:

- The comprehensive experimental design results indicate that material conveying efficiency is maximized when the curvature is 2.03 and the air-to-feed ratio is 4.571 for a rectangular pipe. Combined with the simulation results, this parameter combination ensures more uniform material transportation, meeting operational requirements.
- The CFD-DEM coupled simulation technique employed in this study significantly reduces design resource consumption while achieving ideal results. However, some deviations remain compared to actual tests. Nonetheless, the comparison of simulation and experimental speed measurements shows minimal errors at each point, effectively confirming the reliability of the simulation analysis.

REFERENCES

[1] Afkhami, M., Hassanpour, A., Fairweather, M., & Njobuenwu, D. O. (2015). Fully coupled LES-DEM of particle interaction and agglomeration in a turbulent channel flow. *Computers & Chemical Engineering*, 78, 24-38. doi:10.1016/j.compchemeng.2015.04.003

[2] Alihosseini, M., Saegrov, S., & Thamsen, P.U. (2019). CFD-DEM modelling of sediment transport in sewer systems under steady and unsteady flow conditions. *Water Science and Technology*, 80(11), 2141-2147. doi:10.2166/wst.2020.030

[3] Chen, Q., Xiong, T., Zhang, X., & Jiang, P. (2020). Study of the hydraulic transport of non-spherical particles in a pipeline based on the CFD-DEM. *Engineering Applications of Computational Fluid Mechanics*, 14(1), 53-69. doi:10.1080/19942060.2019.1683075

[4] Cong, H., Zhao, L., Meng, H., Yao, Z., & Wu, Y. (2018). Design and Test of Multilevel Collaborative Drying System for Crop Straws. *Acta Energiae Solaris Sinica*, 39(1), 163-169.

[5] Drescher, E., Mohseni-Mofidi, S., Bierwisch, C., & Kruggel-Emden, H. (2025). A numerical assessment of different geometries for reducing elbow erosion during pneumatic conveying. *Powder Technology*, 449. doi:10.1016/j.powtec.2024.120357

[6] Du, J., Hu, G., Fang, Z., & Fan, Z. (2014). Simulation of dilute pneumatic conveying with bends by CFD-DEM. *Journal of National University of Defense Technology*, 36(4), 134-139.

[7] Ebrahimi, M., & Crapper, M. (2017). CFD-DEM simulation of turbulence modulation in horizontal pneumatic conveying. *Particuology*, 31, 15-24. doi:10.1016/j.partic.2016.05.012

[8] Gao, L., Zhang, W., Du, X., Liu, X., & Yang, J. (2012). Experiment on aerodynamic characteristics of threshed mixtures of peanut shelling machine. *Transactions of the Chinese Society of Agricultural Engineering*, 28(2), 289-292.

[9] Gu, F., Zhao, Y., Wu, F., Hu, Z., & Shi, L. (2022). Simulation analysis and experimental validation of conveying device in uniform rushed straw throwing and seed-sowing Machines using CFD-DEM coupled approach. Computers and Electronics in Agriculture, 193. doi:10.1016/j.compag.2022.106720

[10] Hentschel, A. (2011). Pneumatic conveying and precise metering of dust. *Zkg International*, 64(10), 59-63.

[11] Hilgraf, P. (2023). Direct scaling up of pneumatic conveying tests to industrial systems. *Zkg International*, 76(2), 42-51.

[12] Hongxun, C. K. C. (1993). *Pneumatic conveying device*: Beijing: Machinery Industry Press.

[13] Huo, Z., Zhang, D., Hu, Y., & Pei, X. (2013). Study on the Wear and Pressure Drop of The Pipe Bend in The Pneumatic Conveying of Grain Particles Dilute Phase. *Mechanical Science and Technology for Aerospace Engineering*, 32(11), 1680-1684.

[14] Li, Z., Chen, H., Wu, Y., Xu, Z., Shi, H., & Zhang, P. (2024). CFD-DEM analysis of hydraulic conveying of non-spherical particles through a vertical-bend-horizontal pipeline. *Powder Technology*, 434. doi:10.1016/j.powtec.2024.119361

[15] Liu, F., Li, H., Zhao, X., & Chen, Y. (2024). Study on the Spatiotemporal Evolution Pattern of Frazil Ice Based on CFD-DEM Coupled Method. *Water*, 16(23). doi:10.3390/w16233367

[16] Ma, H., & Zhao, Y. (2018). Investigating the fluidization of disk-like particles in a fluidized bed using CFD-DEM simulation. *Advanced Powder Technology*, 29(10), 2380-2393. doi:10.1016/j.apt.2018.06.017

[17] Ma, Z., Li, Y., & Xu, L. (2011). Testing and analysis on rape excursion components characteristics in floating, friction and wettability. *Transactions of the Chinese Society of Agricultural Engineering*, 27(9), 13-17.

[18] Uzi, A., & Levy, A. (2018). Flow characteristics of coarse particles in horizontal hydraulic conveying. *Powder Technology*, 326, 302-321. doi:10.1016/j.powtec.2017.11.067

[19] Wang, Z., Peng, G., Chang, H., Hong, S., & Ji, G. (2024). Investigation and Improvement of Centrifugal Slurry Pump Wear Characteristics via CFD-DEM Coupling. *Water*, 16(21). doi:10.3390/w16213050

[20] Zhang , D., Zhang , X., Wu , D., Lin , S., Zhang , T., & Xu , W. (2023). Simulation of Pepper Cleaning Based on DEM-CFD Coupling. *Journal of Agricultural Science and Technology*, 25(07), 87-96. doi:10.13304/j.nykjdb.2022.0008

[21] Zhang, X., & Newell, P. (2024). Simulation of Microcapsule Transport in Fractured Media Using Coupled CFD-DEM. *Water Resources Research*, 60(6). doi:10.1029/2023WR035728

[22] Zhao, H., & Zhao, Y. (2020). CFD-DEM simulation of pneumatic conveying n a horizontal pipe. *Powder Technology*, 373, 58-72. doi:10.1016/j.powtec.2020.06.054

[23] Zhao, L., Yu, Z., Zhu, F., Qi, X., & Zhao, S. (2016). CFD-DEM modeling of snowdrifts on stepped flat roofs. *Wind and Structures*, 23(6), 523-542. doi:10.12989/was.2016.23.6.523

[24] Zhou, J.-w., Du, C.-l., Liu, S.-y., & Liu, Y. (2016). Comparison of three types of swirling generators in coarse particle pneumatic conveying using CFD-DEM simulation. *Powder Technology*, 301, 1309-1320. doi:10.1016/j.powtec.2016.07.047